Measuring Earthquake Induced Surface Displacement in Morocco using SBAS Interferometry

Desire Muhire[1] | Yassine Tounsi[1] | Ahmed Siari[1] | Abdelkrim Nassim[*1]
[1]Measurement and Control Instrumentation Laboratory (IMC), Faculty of Sciences, Chouaib Doukkali University, Morocco, nassim.a@ucd.ac.ma (Abdelkrim Nassim)

Abstract

We apply the Small Baseline Subset (SBAS) Differential SAR interferometry (DInSAR) method to monitor ground movement following several earthquakes between 12.09.2015 and 10.03.2016 in Al Hoceïma, Morocco. The study focuses on selecting and stacking multiple interferograms to attenuate the atmospheric noise while preserving the interferometric measurement of the deformation signal. The selection process is discussed to reduce the effect of stacking small signal. We generated 25 interferograms covering the above time span using Sentinel-1 images. Cumulative displacement of -8 to 8 mm was detected in the Rif Mountains and around the epicenter of the 24 February 2004 earthquake.

Keywords

SBAS, Interferometry, Sentinel-1, Earthquakes, Al Hoceïma

Измерение вызванного землетрясением смещения поверхности в Марокко с помощью интерферометрии SBAS

Дезире Муире[1] | Яссин Тоунси[1] | Ахмед Сиари[1] | Абделькрим Нассим[1]
[1]Лаборатория контрольных и измерительных инструментов, факультет естественных наук, университет имени Чуайба Дуккали, Марокко, nassim.a@ucd.ac.ma (Абделькрим Нассим)

Аннотация

Мы применили метод интерферометрии малых базовых линий (SBAS) дифференциальной интерферометрии SAR (DInSAR) для мониторинга смещений поверхности Земли после нескольких землетрясений, произошедших между 12.09.2015 и 10.03.2016 в Эль-Хосейма, Марокко. Основное внимание в исследовании уделяется выбору и сложению нескольких интерферограмм для ослабления атмосферного шума при сохранении интерферометрического измерения сигнала деформации. Обсуждается процесс выбора для уменьшения эффекта сложения в случае слабого сигнала. Мы сгенерировали 25 интерферограмм, охватывающих вышеуказанный промежуток времени, используя изображения Sentinel-1. В горах Риф и вокруг эпицентра землетрясения 24 февраля 2004 года было обнаружено результирующее смещение от -8 до 8 мм.

Ключевые слова

SBAS, интерферометрия, Sentinel-1, землетрясения, Эль-Хосейма

Introduction

Space-based Differential Interferometric Synthetic Aperture Radar (DInSAR) is a remote sensing technique for monitoring surface displacement with millimeter accuracy in the Line of sight (LOS) direction (Massonnet and Feigl, 1998). It has been successfully applied to a wide range of applications such as earthquake-induced deformation detection (Massonnet et al, 1993; Foumelis et al, 2009), crustal deformation (Hunstad et al, 2009), measurement of mining subsidence

* Corresponding author

(Przylucka et al, 2015; Guéguen et al, 2009), and active volcanoes monitoring (Massonnet et al, 1995). In Al Hoceïma, DInSAR was applied to monitor the earthquake-related deformation induced by the 6.4-moment magnitude scale (MW), which occurred on 24 February 2004 (Cakir et al, 2006). The guiding principle of SAR systems relies on the computation of the two-way propagation path of radio waves for topographic measurement. However, the atmospheric medium, defined by a refractive index, induces a path delay which significantly reduces precise measurement (Goldstein, 1995).

The conventional Differential InSAR (DInSAR) has experienced algorithmic advances based on time series analysis to significantly reduce this atmospheric noise. These modern techniques can be categorized into two distinct groups, namely the Persistent Scatterer InSAR (PS-InSAR) (Ferretti et al, 2000) and Small Baseline Subset SAR interferometry (SBAS) (Berardino et al, 2002). The SBAS was utilized for its robustness and better estimation of surface deformation in non-urban territories. The remainder of the paper is organized as follows: section II introduces the region of study, section III presents methods, section IV embodies results and discussions, and section V concludes.

Region of study

Al Hoceïma, Morocco, is located at 35 ◦ 14 ’57 "north, 3 ◦ 55’ 58" west on the eastern range of the Rif mountain near the Alboran Sea. Al Hoceïma has a dynamic seismic activity resulting from the convergence of African and Eurasian tectonic plates. This motion causes major earthquakes, such as the 6.4 Mw earthquake (Goldstein, 1995; Tahayt et al, 2009; Kariche et al, 2018), on February 24, 2004, resulting in more than 630 deaths (Figure 1 and 2); and recently, a 6.3 Mw on January 25, 2016 (Figure 1), followed by several aftershocks felt in the region, according to United States Geological Survey (USGS) data (Figure 1, 2a and 2b) (Kariche et al, 2016).

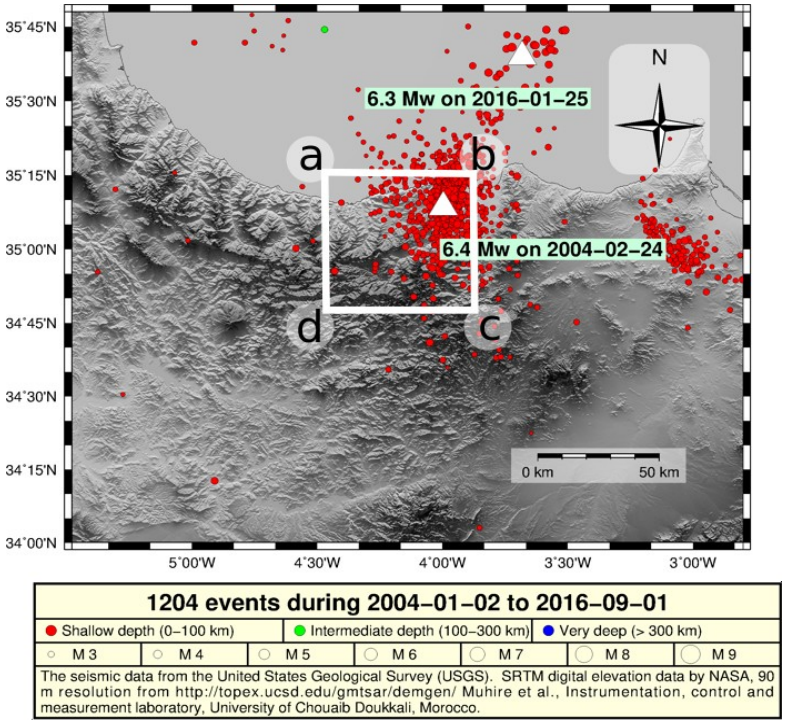

Figure. 1. Al Hoceïma seismic activity recorded by USGS on the 6.4 and 6.3 Mw earthquakes respectively on February 24, 2004, and January 25, 2016. The region of study is indicated by the [a, b, c, d] rectangle. The Shuttle Radar Topography Mission (SRTM) Digital Elevation Model (Farr and Kobrick, 2000) and the Generic Mapping Tools (Wessel and Smith, 1998) have been used to generate this map.

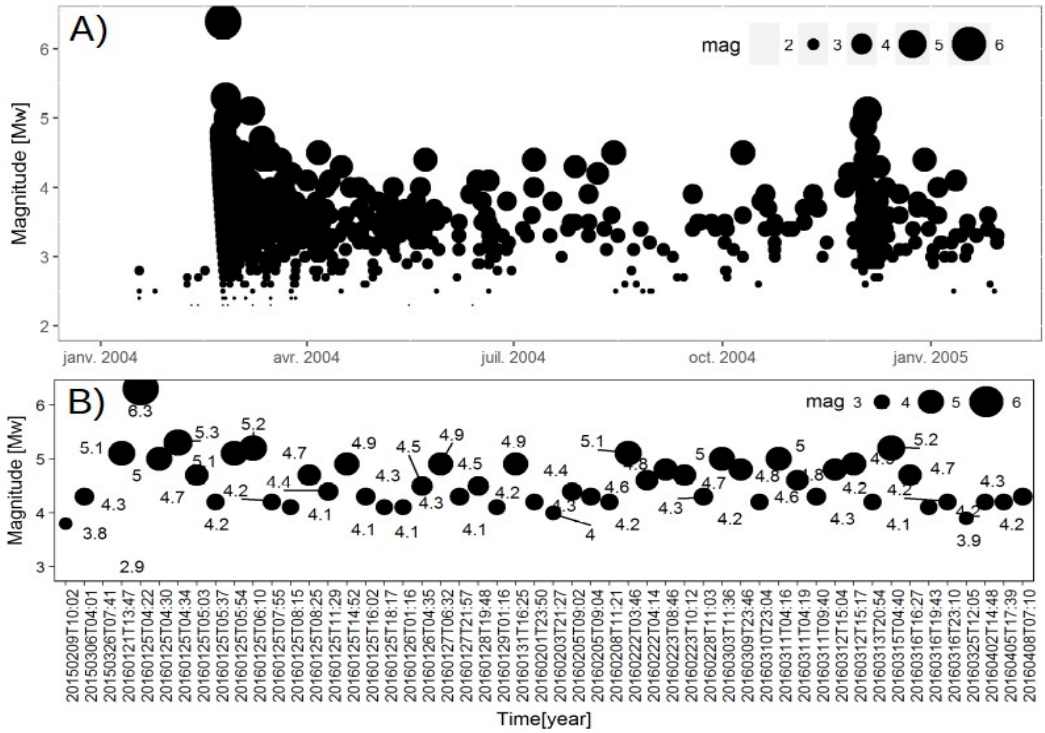

Figure 2: The temporal observation of the Al Hoceïma seismic activity with respect to the 6.4 and 6.3 Mw earthquakes.

Region of study

Sentinel-1 Satellite Imagery

Sentinel-1 is a constellation of two European Space Agency (ESA) C-band (S1-A and B) Synthetic Aperture Radar (SAR) missions in the Copernicus program (Geudtner and Torres, 2012). S1-A launched in 2014 in Interferometric Wide swath (IW) mode with a revisit time of 12 days and 5 m by 20 m spatial resolution has been used in this work. The selection of S1-IW image has been systematically used to exploit the short revisit satellite time of Sentinel-1 Radar in the period prior the earthquake of 6.3 Mw on January 25, 2016, and its aftershock (figure 1, 2). In a seismic case, a short revisit time permits the acquisition of several and sufficient images for Time series Differential InSAR (TInSAR) analysis while staying in the period of the earthquake and its aftershock.

The data selection was conducted with respect to ground USGS data (figure 1). The numbers of the radar images toward the starting were 18 images. To remain in the problematic posed, that of isolating the measures to the strong earthquake on January 25, 2016, we selected images with ground USGS data demonstrates significant estimations. In the presented framework, the USGS data from the period of February 09, 2015 to March 06, 2015 that indicates a light earthquake has been removed to avoid transient temporal decorrelations with respect to the date of the strong earthquake.

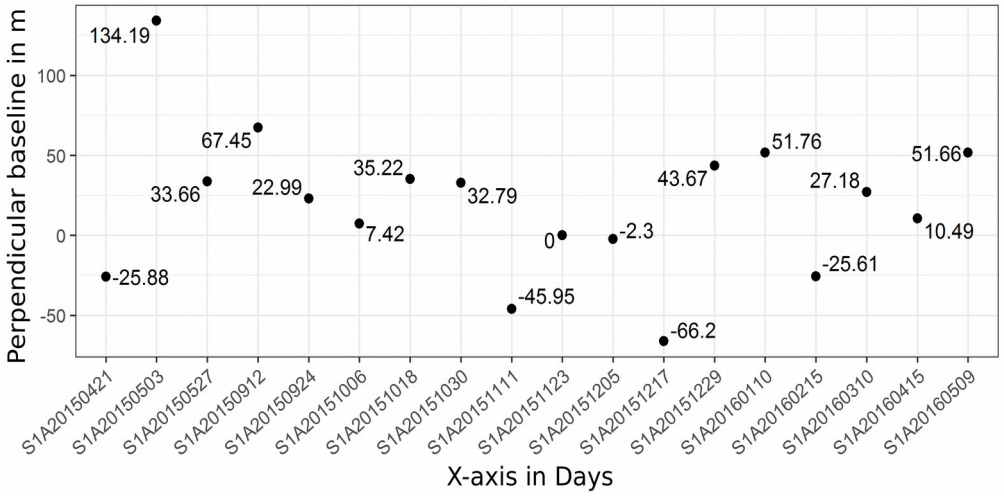

Figure 3: Sentinel-1 data from April 21, 2015 to May 09, 2016 have been downloaded from ESA to monitor earthquakes observed from ground measured data starting from September 02, 2015 to April 08, 2016.

The USGS data (figure 2) also showed non-significant ground measurement form March 06,

2015, to January 21, 2016. However, we have systematically included acquisitions from September 21, 2015, to achieve the minimum number of images required for atmospheric noise attenuation. Further SAR images have been removed from a practical point of view or by the selection process of the master and interferometric pairs (figure 4).

Pair selection approach

The proposed pair selection approach is based on the relationship of the coherence and the phase variance error by Rodriguez and Martin (Rodriguez and Martin, 1992; Fielding et al, 2005; Grandin et al, 2016). In principle, the stacking approaches are based on averaging N independent observations (looks or interferograms) to mitigate the atmospheric signals to $1/\sqrt{N}$ fold (Ferretti et al, 2000; Zebker et al, 1997; Sandwell and Price, 1998). However, the determination of the minimum required is not mathematically well defined in literature for SBAS and PSInSAR (Ferretti et al, 2000; Zebker et al, 1997; Sandwell and Price, 1998) or Stanford Method for Persistent Scatterers (STAMPS) (Hooper et al, 2012). In this subsection, we discuss the use of the coherence and the phase variance relation to define commonly used thresholding coherence value and the number of interferograms in stacking methods (Ferretti et al, 2000; Zebker et al, 1997; Sandwell and Price, 1998) in the seismic case.

The phase variance and coherence relation are given as Rodriguez and MartinRodriguez and Martin (Rodriguez and Martin, 1992; Fielding et al, 2005; Grandin et al, 2016):

$$\sigma_{\phi}^{2} = \frac{1}{2N\gamma^{2}}\left(1-\gamma^{2}\right) \qquad (1)$$

Where σ_{ϕ}, γ, N are respectively the standard deviation, the coherence and N the number of observations (figure 3).

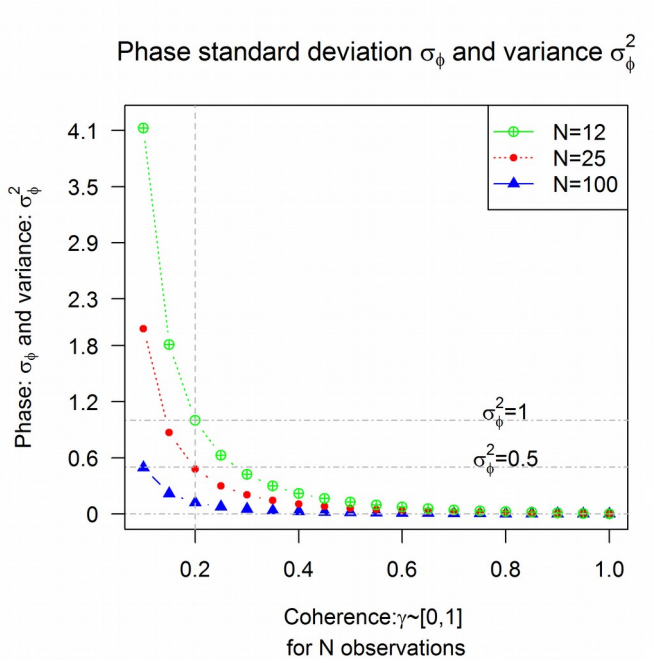

Figure 4: The plotting of the equation for representing the phase variance error as a function of the coherence and the number of independent phase observations.

On one hand, we can observe, from figure (3), that the phase variance error tends toward infinity for low coherence for any given number of observation and rapidly drops for coherence values below 0.2. Thus, this relation $(eq.1)$ can demonstrate that the value 0.2 coherence generally used in literature (Berardino et al, 2002) for thresholding is a good start in reducing phase variance error. On the other hand, increasing of the number of looks or phase observations reduces the phase variance. However, as discussed above, stacking an elevated number of interferogram reduces the resolution and presents the risk of not measuring small amplitude signal, such in the case of seismic deformation.

From the expression $(eq.1)$, a complementary approach can be taken by increasing a high constrain on coherence while setting the minimum required N looks to obtain one can obtained low phase error (figure 4). A high value of coherence, not only reduce the phase variance, error, it also reduces phase unwrapping error propagation and also fasten this process. The figure shows that the number of interferogram $N \cong 25$ used generally as the minimum required observation (Ferretti et al, 2000; Zebker et al, 1997; Sandwell and Price, 1998) present low phase variance inferior to 0.5 as compared to the $N \cong 25$. Considering the seismic case, we generated a critical minimum number of interferogram for InSAR time series of 25 interferograms with a minimum of $\gamma = 0.3$ via the short baseline subset network (Farr and Kobrick, 2000) (figure 5).

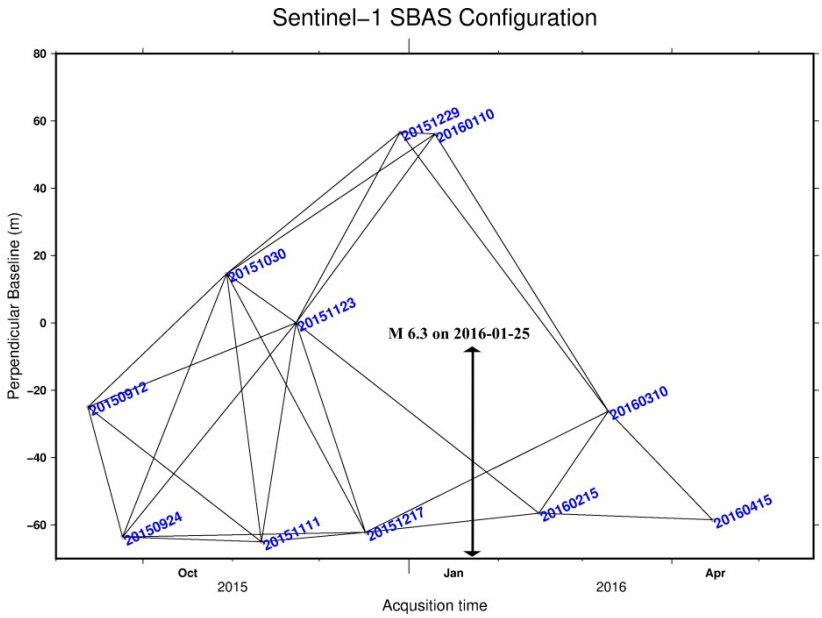

Figure 5: The SBAS network is defined by selecting a 90 days temporal and a 100 m spatial perpendicular baseline.

Data processing

The repeat-pass interferometry applied on two SAR images generates an interferogram that contains the topography, the noise, and the deformation with respect to their acquisition's dates (Massonnet and Feigl, 1998). The topographic component can be subtracted by the conventional Differential InSAR (DInSAR) using an external Digital Elevation Model (DEM). The Small Baseline Subset approach (SBAS) (Berardino et al, 2002) is an empirical method that uses a multitude of differential SAR interferograms and generally linear inversion to mitigate the atmospheric noise.

The DInSAR was applied to several SAR Sentinel-1 data acquired from September 21, 2015 to April 8, 2016 (Figures 2 and 6.A) covering earthquakes observed from January 21, 2016 to April 8, 2016.

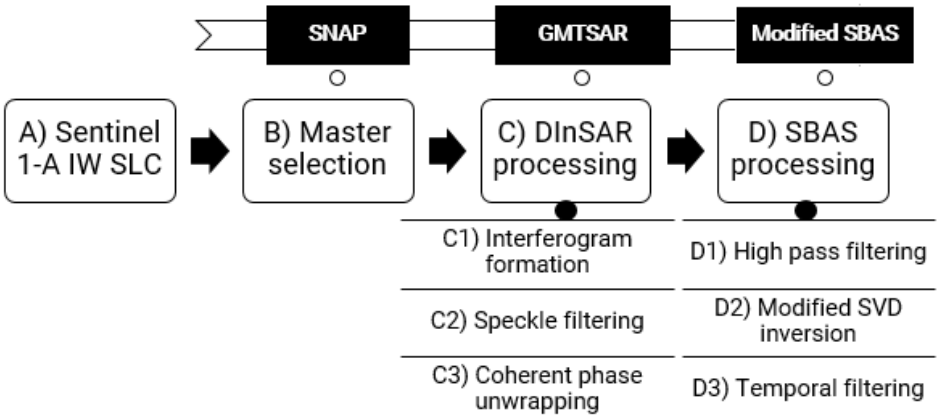

Figure 6: The proposed the Small Baseline Subset (SBAS) algorithm approach.

The DInSAR has been proceeded to form differential interferogram from single-look complex (SLC) SAR images following the proposed approach (figure 6). The selection of the master was performed to minimize the spatial perpendicular baseline and the temporal baseline, as well as the mean doppler centroid frequency difference from the critical values. These critical values are utterly based on SAR metadata and are used to define a modeled cost function in the form of coherence. This modeled coherence is calculated in the Sentinel Application Platform (SNAP) (Zuhlke et al. 2015). However, the rest of the DInSAR process is conducted using the Generic Mapping Tools InSAR Processing System(GMTSAR)[22] (Sandwell et al, 2010). All SAR slaves were coregistered to the one master defined (figure 6.B and 6.C1), also called super master for multiple Interferogram formations; and for our data, it is was acquired on November 23, 2015 (figure 3 and 4). The removal of flat Earth from satellite orbit and topographic phase removal using the Shuttle Radar Topography Mission (SRTM 3-arc-second) the digital elevation model (DEM) (Farr and Kobrick, 2000) subtraction were resumed in the processing chain (figure 6) as interferogram formation(figure 6.C1). The coherence weighted adaptive filter of Goldstein using sliding windows in the frequency domain (figure 6.C2) was applied to wrapped interferogram (Baran et al, 2003).

A coherent phase unwrapping, referred in (figure 6.C3), is applied on the wrapped phase interferogram to mask decorrelating pixels and the correlating pixels are interpolated, and an interpolation is applied to obtain a continuous spatially dense map. The absolute differential phase interferogram was then recovered via the Statistical-Cost, Network-Flow Algorithm for Phase Unwrapping (SNAPHU) (Chen and Zebker, 2000). The modified SBAS approach (figure 6, D) by (Grandin et al, 2016) is applied for atmospheric correction high pass filtering of spatially correlated and long waves atmospheric and orbital ramp in the unwrapped phase interferogram.

Results and discussions

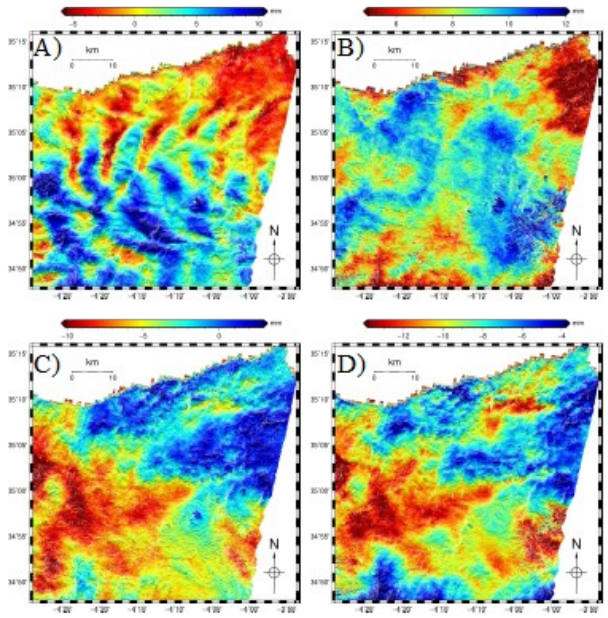

Figure 7: A sample of 4 differential interferograms, (a) 20151030-20160110, (b) 20151123-20160215,(c) 20151229-20160310 and (d) 20160215-20160310, measured from GMTSAR. They contain atmospheric noise, orbit and, topographic error. Other interferograms have been omitted for clarity.

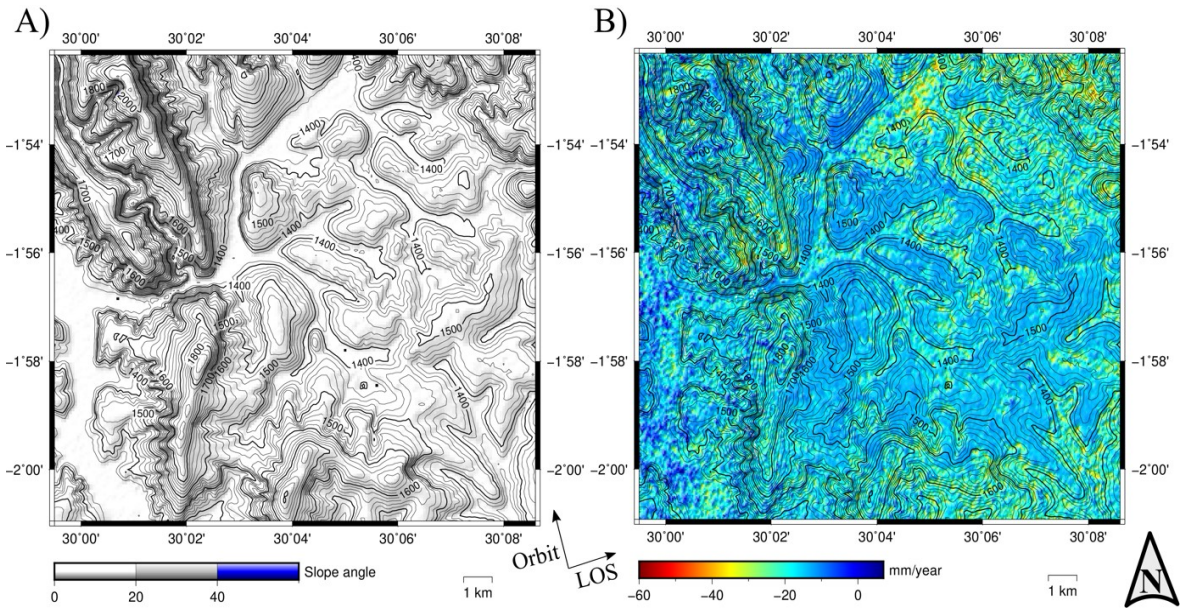

Figure 8: Cumulative displacement of Al Hoceïma using the SBAS approach applied to the Sentinel-1 images.

The purpose of this work was to measure the surface deformation induced by the Al Hoceïma earthquake of 6.3 Mw (USGS) on January 25, 2016. The extensive geophysical studies on the

seismic assessment and interpretation can be found in (Cakir et al, 2006; Kariche et al, 2017; Tahayt et al, 2009). The results (figure 7) obtained from the region of study (figure 1) show a deformation detected in the north-east, around the location of the epicenter of February 24, 2004, 6.4 Mw, and in the south-west in the mountains of Rif (figure 1).

Conclusion

We have applied the SBAS interferometry approach for the measurement of deformation due to the Al Hoceïma seismic. The purpose of this approach was to take advantage of the millimetric resolution and the short spatiotemporal baseline of the Sentinel-1 images covering the region of study to observe its dynamic due to a series of earthquakes. The proposed approach was to select an optimum number of interferograms to avoid attenuating the deformation signal by stacking. We have noticed cumulative displacement within a range of -8 mm and 8 mm obtained from 25 Interferograms using the SBAS approach applied on the Sentinel-1 images of AL Hoceïma. Small deformation signal was detected in the north-east, around the location of the epicenter of February 24, 2004, 6.4 Mw and in the south-west in the mountains of Rif.

References

D. Massonnet and K. L. Feigl (1998) *Radar interferometry and its application to changes in the Earth's surface*, Rev. Geophys., vol. 36, no. 4, pp. 441–500.

D. Massonnet et al (1993) *The displacement field of the Landers earthquake mapped by radar interferometry*, Nature, vol. 364, no. 6433, p. 138.

M. Foumelis, I. Parcharidis, E. Lagios, and N. Voulgaris (2009) *Evolution of post-seismic ground deformation of the Athens 1999 earthquake observed by SAR interferometry*, J. Appl. Geophys., vol. 69, no. 1, pp. 16–23.

I. Hunstad, A. Pepe, S. Atzori, C. Tolomei, S. Salvi, and R. Lanari (2009) *Surface deformation in the Abruzzi region, Central Italy, from multitemporal DInSAR analysis*, Geophys. J. Int., vol. 178, no. 3, pp. 1193–1197.

M. Przylucka, G. Herrera, M. Graniczny, D. Colombo, and M. Béjar-Pizarro (2015) *Combination of conventional and advanced DInSAR to monitor very fast mining subsidence with TerraSAR-X data: Bytom City (Poland)*, Remote Sens., vol. 7, no. 5, pp. 5300–5328.

Y. Guéguen et al. (2009) *Monitoring residual mining subsidence of Nord/Pas-de-Calais coal basin from differential and Persistent Scatterer Interferometry (Northern France)*, J. Appl. Geophys., vol. 69, no. 1, pp. 24–34.

D. Massonnet, P. Briole, and A. Arnaud. (1995) *Deflation of Mount Etna monitored by spaceborne radar interferometry*, Nature, vol. 375, no. 6532, p. 567.

Z. Cakir, M. Meghraoui, A. M. Akoglu, N. Jabour, S. Belabbes, and L. Ait-Brahim (2006) *Surface deformation associated with the Mw 6.4, 24 February 2004 Al Hoceima, Morocco, earthquake deduced from InSAR: Implications for the active tectonics along North Africa*, Bull. Seismol. Soc. Am., vol. 96, no. 1, pp. 59–68.

R. Goldstein (1995) *Atmospheric limitations to repeat-track radar interferometry*, Geophys. Res. Lett., vol. 22, no. 18, pp. 2517–2520.

A. Ferretti, C. Prati, and F. Rocca (2000) *Nonlinear subsidence rate estimation using permanent scatterers in differential SAR interferometry*, IEEE Trans. Geosci. Remote Sens., vol. 38, no. 5, pp. 2202–2212.

P. Berardino, G. Fornaro, R. Lanari, and E. Sansosti (2002) *A new algorithm for surface deformation monitoring based on small baseline differential SAR interferograms*, IEEE Trans. Geosci. Remote Sens., vol. 40, no. 11, pp. 2375–2383.

T. G. Farr and M. Kobrick (2000) *Shuttle Radar Topography Mission produces a wealth of data*, Eos Trans. Am. Geophys. Union, vol. 81, no. 48, pp. 583–585.

P. Wessel and W. H. Smith (1998) *New, improved version of Generic Mapping Tools released*, Eos Trans. Am. Geophys. Union, vol. 79, no. 47, pp. 579–579.

D. Geudtner and R. Torres (2012) *Sentinel-1 system overview and performance*, in 2012 IEEE International Geoscience and Remote Sensing Symposium, pp. 1719–1721.

E. Rodriguez and J. M. Martin (1992) *Theory and design of interferometric synthetic aperture radars*, IEE Proc. F Radar Signal Process.

E. J. Fielding et al. (2005) *Surface ruptures and building damage of the 2003 Bam, Iran, earthquake mapped by satellite synthetic aperture radar interferometric correlation*, J. Geophys. Res. Solid Earth, vol. 110, no. 3, pp. 1–15.

R. Grandin, E. Klein, M. Métois, and C. Vigny (2016) *Three-dimensional displacement field of the 2015 Mw8. 3 Illapel earthquake (Chile) from across-and along-track Sentinel-1 TOPS interferometry*, Geophys. Res. Lett., vol. 43, no. 6, pp. 2552–2561.

H. A. Zebker, P. A. Rosen, and S. Hensley (1997) *Atmospheric effects in interferometric*

synthetic aperture radar surface deformation and topographic maps, J. Geophys. Res. Solid Earth, vol. 102, no. B4, pp. 7547–7563.

D. T. Sandwell and E. J. Price (1998) *Phase gradient approach to stacking interferograms*, J. Geophys. Res. Solid Earth, vol. 103, no. B12, pp. 30183–30204.

A. Hooper, D. Bekaert, K. Spaans, and M. Arıkan (2012) *Recent advances in SAR interferometry time series analysis for measuring crustal deformation*, Tectonophysics, vol. 514–517, pp. 1–13.

M. Zuhlke et al. (2015) *SNAP (sentinel application platform) and the ESA sentinel 3 toolbox*, in Sentinel-3 for Science Workshop, vol. 734.

D. T. Sandwell, R. J. Mellors, X. Tong, M. Wei, and P. Wessel (2010) *GMTSAR software for rapid assessment of earthquakes*, in AGU Fall Meeting Abstracts.

I. Baran, M. P. Stewart, B. M. Kampes, Z. Perski, and P. Lilly (2003) *A modification to the Goldstein radar interferogram filter*, IEEE Trans. Geosci. Remote Sens., vol. 41, no. 9, pp. 2114–2118.

C. W. Chen and H. A. Zebker (2000) *Network approaches to two-dimensional phase unwrapping: intractability and two new algorithms*, JOSA A, vol. 17, no. 3, pp. 401–414.

J. Kariche, M. Meghraoui, Y. Timoulali, E. Cetin, and R. Toussaint (2017) *The Al Hoceima earthquake sequence of 1994, 2004 and 2016: Stress transfer and poroelasticity in the Rif and Alboran Sea region*, Geophys. J. Int., vol. 212, no. 1, pp. 42–53.

A. Tahayt et al. (2009) *The Al Hoceima (Morocco) earthquake of 24 February 2004, analysis and interpretation of data from ENVISAT ASAR and SPOT5 validated by ground-based observations*, Remote Sens. Environ., vol. 113, no. 2, pp. 306–316.

J. Kariche, M. Meghraoui, Y. Timoulali, E. Cetin, and R. Toussaint (2018) *The Al Hoceima earthquake sequence of 1994, 2004 and 2016: Stress transfer and poroelasticity in the Rif and Alboran Sea region*, Geophys. J. Int., vol. 212, no. 1, pp. 42–53.

J. Kariche, M. Meghraoui, Y. Timoulali, E. Cetin, and R. Toussaint (2016) *The Alboran Sea earthquake (Mw 6 .3) of 25 January 2016 : A consequence of the 1994-2004 Al Hoceima seismic events?*, in 35th General Assembly of the European Seismological Commission, no. January, p. 2016.